Aging Brain 5 (2024) 100114

Contents lists available at ScienceDirect

Aging Brain

journal homepage: www.elsevier.com/locate/nbas

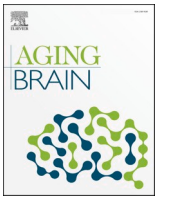

Intrinsic functional connectivity strength of SuperAgers in the default mode and salience networks: Insights from ADNI

Haley E. Keenan [a], Alexis Czippel [d], Sepideh Heydari [d], Jodie R. Gawryluk [d,e,f], Erin L. Mazerolle [a,b,c,*], for the Alzheimer's Disease Neuroimaging Initiative [1]

[a] Department of Psychology, St. Francis Xavier University, 4130 University Avenue, Antigonish, NS B2G 2W5, Canada
[d] Department of Psychology, University of Victoria, 3800 Finnerty Road, Victoria, BC V8P 5C2, Canada
[e] Institute on Aging and Lifelong Health, University of Victoria, 3800 Finnerty Road, Victoria, BC V8P 5C2, Canada
[f] Division of Medical Sciences, University of Victoria, 3800 Finnerty Road, Victoria, BC V8P 5C2, Canada
[b] Department of Computer Science, St. Francis Xavier University, 4130 University Avenue, Antigonish, NS B2G 2W5, Canada
[c] Department of Biology, St. Francis Xavier University, 4130 University Avenue, Antigonish, NS B2G 2W5, Canada

ARTICLE INFO

Keywords:
Successful aging
SuperAging
Functional connectivity
Default mode network
Salience network

ABSTRACT

There exists a group of older individuals who appear to be resistant to age-related memory decline. These "SuperAgers" have been shown to demonstrate preservation of cortical thickness and functional connectivity strength across the cortex which positively correlates with memory performance. Over the last decade, roughly 30 articles have been published regarding SuperAgers; however, to our knowledge, no replications of these studies have been published. The current study sought to conceptually replicate Zhang and colleagues' (2020) findings that SuperAgers demonstrate stronger intrinsic functional connectivity within the default mode (DMN) and salience networks (SN), and that connectivity strength within these networks correlates with memory performance. We identified 20 SuperAgers and 20 matched Normal Agers in the control cohort of the Alzheimer's Disease Neuroimaging Initiative (ADNI) database. We compared the functional connectivity strength of the DMN and SN between these groups, and used the Rey Auditory Verbal Learning Test (RAVLT) to evaluate correlations between functional connectivity and memory performance. Our results did not replicate Zhang and colleagues'

Abbreviations: DMN, default mode network; SN, salience network; FC, functional connectivity; ADNI, Alzheimer's Disease Neuroimaging Initiative; ROI, region-of-interest; MRI, magnetic resonance imaging; PET, positron emission tomography; MCI, mild cognitive impairment; AD, Alzheimer's disease; CVLT, California Verbal Learning Test; RAVLT, Rey Auditory Verbal Learning Test; TMT-B, Trail Making Test part B; MPRAGE, magnetization-prepared rapid gradient echo; EPI, echo-planar imaging; FSL, FMRIB Software Library; BET, Brain Extraction Tool; CSF, cerebrospinal fluid; FDR, false discovery rate; MNI, Montreal Neurological Institute; QUADAS-2, Quality Assessment of Diagnostic Accuracy Studies-2; PCC, posterior cingulate cortex; mPFC, medial prefrontal cortex; IPL, inferior parietal lobule; HF, hippocampal formation; AI, anterior insula; ACC, anterior cingulate cortex; MCC, midcingulate cortex; SFG, superior frontal gyrus; aMTG, anterior middle temporal gyrus; vlPFC, ventrolateral prefrontal cortex; pgACC, pregenual anterior cingulate cortex; sgACC, subgenual anterior cingulate cortex; AG, angular gyrus; dmPFC, dorsomedial prefrontal cortex; rmPFC, rostromedial prefrontal cortex; SMG, supramarginal gyrus; aMCC, anterior midcingulate cortex; FOV, field of view; TE, echo time; TR, repetition time; TI, inversion time.

* Corresponding author at: Department of Psychology, St. Francis Xavier University, Antigonish, NS B2G 2W5, Canada.
E-mail address: emazerol@stfx.ca (E.L. Mazerolle).

[1] Data used in preparation of this article were obtained from the Alzheimer's Disease Neuroimaging Initiative (ADNI) database (https://adni.loni.usc.edu). As such, the investigators within the ADNI contributed to the design and implementation of ADNI and/or provided data but did not participate in analysis or writing of this report. A complete listing of ADNI investigators can be found at: http://adni.loni.usc.edu/wp-content/uploads/how_to_apply/ADNI_Acknowledgement_List.pdf.

https://doi.org/10.1016/j.nbas.2024.100114
Received 8 September 2023; Received in revised form 12 January 2024; Accepted 11 March 2024
Available online 21 March 2024

(2020) results, as we found negligible differences between SuperAgers and Normal Agers in the DMN and SN, and no significant correlations between functional connectivity and memory performance after accounting for multiple comparisons. More replications are needed to confirm existing work. In addition, more research with larger SuperAger samples and more consistent definitions of SuperAging is needed, so that we can better understand this remarkable group of older adults.

Introduction

Normal aging typically involves a decline in memory performance across multiple domains [23]. Recent research has identified a group of older individuals who appear to be resistant to age-related episodic memory decline. Research into these "SuperAgers" has reported youthful episodic memory performance and anatomical and functional differences in the brain compared to their cognitively average, "Normal Aging", peers.

SuperAgers can be loosely defined as older individuals (ages 60–80 +) who perform in the range of young or middle-aged adults on measures of episodic memory, and are otherwise cognitively normal (see discussion for more information on SuperAging definitions). SuperAging research is attempting to identify genetic, physiological, and lifestyle differences between these individuals and Normal Agers to determine what mechanisms are responsible for SuperAgers' resistance to cognitive decline [12]. Harrison and colleagues (2012) were the first to note that SuperAgers do not show typical age-related atrophy in the brain. In addition to demonstrating comparable cortical thickness to middle-aged controls across numerous brain regions, SuperAgers also demonstrated greater cortical thickness in the anterior cingulate cortex [25]. Subsequent studies have supported the finding that SuperAgers demonstrate greater cortical thickness than typical older adults in the anterior and middle cingulate cortex [9,24,53] and that the cingulate cortex of SuperAgers is thicker than or indistinguishable from younger control groups [19]. There is also longitudinal evidence that left hemisphere regions of greater cortical thickness in SuperAgers also thins at a slower rate compared to typical older adults, suggesting preservation of cortical thickness in SuperAgers [9,24].

Several of the cortical regions that show less atrophy in SuperAgers lie within two functional brain networks [12]. The default mode network (DMN) is characterized by activation during periods of rest and wakeful reflection, and deactivation during task performance [22,35,41,48]. The DMN includes the posterior cingulate cortex (PCC)/precuneus, medial prefrontal cortex (mPFC), inferior parietal lobule (IPL), hippocampal formation (HF), and several more regions [8,22,41,48]. Aging has a detrimental effect on default mode functioning. Many studies have found age-related declines in within-network DMN functional connectivity (FC) strength [1,6,10,15,33,38,62] (but see [57]). The exact function of the DMN is not known, but it has been speculated to monitor the external environment and mediate internal thought [8]. Pertaining to memory, studies have linked default mode activity to both memory encoding (regions: IPL, precuneus, PCC, ventromedial PFC, superior and middle frontal gyrus, and superior temporal gyrus) [26,27] and retrieval (regions: angular gyrus, PCC, IPL, precuneus, anterior PFC) [46,47], and strength of DMN FC has been found to positively predict memory performance [51,58,59].

The salience network (SN) monitors internal and external environments for salient information, then coordinates the activation/deactivation of other brain networks for subsequent processing and response [36,44,45]. When the SN detects stimuli that need attention, it signals to switch off the DMN and for control networks to take over [21,50]. Its hubs are in the anterior insula (AI) and the anterior cingulate cortex (ACC), and it includes cortical nodes in the midcingulate cortex (MCC) and temporal pole, as well as several subcortical nodes [36,44,45,54]. Similar to the DMN, SN FC strength has also been shown to weaken with age [33,38,39] (but see [57]) and FC strength within this network has been found to be positively correlated with memory performance [61].

Zhang and colleagues (2020) investigated the strength of SuperAgers' intrinsic FC within the DMN and SN, and the correlation between FC strength and memory performance. After identifying a sample of 17 SuperAgers, 23 Normal Agers, and 41 young-adult controls, the researchers performed seed-based voxelwise and region-of-interest (ROI) FC analyses of the DMN and SN to identify regions where SuperAgers showed stronger FC compared to Normal Agers. They found that SuperAgers demonstrated stronger FC within the DMN and SN compared to Normal Agers, and statistically indistinguishable FC strength from young adults, at the voxel level (DMN: from the seed region in the right PCC to the right HF, left superior frontal gyrus (SFG), right anterior middle temporal gyrus (aMTG), right ventrolateral prefrontal cortex (vlPFC), right pregenual anterior cingulate cortex (pgACC), right subgenual anterior cingulate cortex (sgACC), and bilateral angular gyrus (AG), dorsomedial prefrontal cortex (dmPFC), and rostromedial prefrontal cortex (rmPFC); SN: from the right dorsal anterior insula (dAI) seed to the right supramarginal gyrus (SMG) and bilateral anterior midcingulate cortex (aMCC)). Lastly, they found that FC strength in all seed-target pairs within these networks positively predicted memory performance.

The current study is a conceptual replication of Zhang and colleagues (2020), which found that SuperAgers have stronger FC within the DMN and SN compared to Normal Agers, and that stronger FC in these networks is correlated with superior memory performance. We hypothesized that our sample, derived from the ADNI database, would show similar group differences in connectivity strength as those reported in Zhang and colleagues (2020) and FC strength would positively predict memory performance.

Methods

Alzheimer's Disease Neuroimaging Initiative

Data used in this article were obtained from the ADNI database (adni.loni.usc.edu). ADNI was launched in 2003 as a public–private partnership, led by Principal Investigator Michael W. Weiner, MD. The primary goal of ADNI has been to test whether serial magnetic resonance imaging (MRI), positron emission tomography (PET), other biological markers, and clinical and neuropsychological assessment can be combined to measure the progression of mild cognitive impairment (MCI) and early Alzheimer's disease (AD). For up-to-date information, see https://www.adni-info.org.

Participant Selection

All ADNI participants provided informed written consent approved by each sites' Institutional Review Board. Secondary data use for the current study was approved by the Human Research Ethics Board at the University of Victoria, in British Columbia, Canada. Selection criteria was restricted to ADNI participants aged 60 and over within the control cohort who had resting-state functional MRI (rs-fMRI) scans and T1-weighted anatomical scans. According to ADNI screening procedures, controls were free of memory complaints, showed an absence of significant impairment in cognitive functioning and everyday living, and memory function was normal (assessed using the Logical Memory II Subscale from the Wechsler Memory Scale, Mini-State Mental Exam, and Clinical Dementia Rating). For more information on ADNI screening procedures and group classification, see ADNI's procedures manuals [2–3]. For inclusion in the current study, participants' cognitive test scores were required to meet criteria for SuperAging or Normal Aging (detailed below). For participants who had multiple scans available, their first scan was used for analysis. The cognitive test scores closest to a participant's first fMRI scan date were used to determine group membership.

SuperAging and Normal Aging Definitions

The SuperAging and Normal Aging definitions for this study were adapted from Zhang et al. [61]. With regards to age range, Zhang and colleagues (2020) included participants between the ages of 60 and 80. The cognitive tests used to classify SuperAgers and Normal Agers were based on previous studies of SuperAging [20,19,18,17,25,42]. Zhang et al. [61] used the California Verbal Learning Test (CVLT) [13] as their measure of semantic memory; however, we used the Rey Auditory Verbal Learning Test (RAVLT) [43], as it is included in the ADNI database and is also used in several SuperAging studies. The Trail Making Test part B (TMT-B) [56] was used to measure non-memory cognitive performance, as per Zhang et al. [61] and other SuperAging studies. Zhang et al. used the long-delay free recall memory score from the CVLT in their SuperAging definition; however, no delayed recall score is available on ADNI. Instead, ADNI includes an immediate score (the sum of words recalled after the five learning trials) and a forgetting score (the number of words recalled after the last learning trial minus the words recalled after the 30-minute delay). Normative data for the RAVLT from Strauss et al. [52] includes norms for the words recalled after each learning trial, words recalled after the delay, and the sum of words recalled

Table 1
Participant Demographic Information and Cognitive Test Data.

	SuperAgers (n = 20)	Normal Agers (n = 20)	p-value
Sex			
Female, n (%)	15 (75)	15 (75)	
Male, n (%)	5 (25)	5 (25)	
Ethnicity			
Non Hispanic/Latino White, n (%)	16 (80)	19 (95)	
Hispanic/Latino, n (%)	1 (5)	0 (0)	
Indian/Alaskan, n (%)	1 (5)	0 (0)	
Asian, n (%)	2 (10)	0 (0)	
Black, n (%)	0 (0)	1 (5)	
Scanner Manufacturer			
Philips, n (%)	3 (15)	3 (15)	
Siemens, n (%)	13 (65)	13 (65)	
GE, n (%)	4 (20)	4 (20)	
Age, M (SD) range	72.1 (6.8) 64.9–87.8	72.1 (7.0) 62.1–86.4	0.971
Education, M (SD) range	17.6 (1.6) 14–20	16.9 (2.0) 14–20	0.229
Days between fMRI and cognitive testing	15.4 (23.1) 0–96	40.3 (35.5) 3–135	0.013
RAVLT-I, M (SD) range	61.7 (4.5) 57–74	41.3 (5.7) 32.50	0.000*
RAVLT-F, M (SD) range	0.2 (0.8) −2–1	2.8 (1.9) 0–6	0.000*
TMT-B, M (SD) range	56.7 (15.3) 37–87	72.4 (21.3) 49–125	0.000*

Note. Scanner types included Philips Medical Systems, Siemens, or GE Medical Systems. Age and education are given in years. RAVLT immediate score (RAVLT-I) is the sum of words recalled on all learning trials. RAVLT forgetting score (RAVLT-F) is the number of words recalled on trial five minus words recalled after a 30-minute delay. Trail Making Test part B (TMT-B) is the number of seconds it took to complete the task. Two-sample t-test p-value (2-tailed).
*$p < 0.05$.

during the learning trials. Therefore, the immediate score was compared to the norms for the words recalled during the learning trials, but the forgetting score could not be directly compared to these norms. Instead, the forgetting score was compared to the difference between the means for the delayed trial normative data and trial five normative data [52], Table 10–61). This difference represents the number of words forgotten by the participants in the normative database. As such, we essentially examined delayed recall in SuperAgers relative to norms of young adults.

SuperAgers were defined as individuals ages 60 and over who met the following three criteria: First, an ADNI RAVLT immediate score at or above the normative mean for young adults (ages 20–29 years old; Table 10-61 in [52]). Second, an ADNI RAVLT forgetting score no higher than one standard deviation of the difference between the normative means for the delayed trial and trial five for young adults (Table 10-61 in [52]). Third, an ADNI TMT-B score within one standard deviation of, or lower than, the normative mean for their age group and years of education (Table 2 in [56]). The TMT-B measures processing speed and the score reflects the number of seconds it took the participant to complete the task.

Normal Agers were defined as individuals aged 60 and above who obtained an ADNI RAVLT immediate score within one standard deviation of the normative score for their age group [52], Table 10–61), an ADNI RAVLT forgetting score within one standard deviation of the difference between the means for the delayed trial and trial five for their age group [52], Table 10–61), and an ADNI TMT-B score within one standard deviation or lower than the mean for their age group and years of education (Table 2 in [56]).

Case Matching

A total of 35 SuperAgers (28 female, mean age 71.9) and 94 Normal Agers (41 female, mean age 76.0) were identified according to the criteria. Normal Agers were case matched to SuperAgers based on age (±five years), sex, years of education (±two years), scan date (±five years), and MRI manufacturer. Twenty-five SuperAging and Normal Aging pairs were successfully matched. Ten SuperAgers did not have a Normal Aging pair that fell within the matching criteria. Five further pairs were excluded due to artifacts or missing data in the images of at least one member of the pairs (four SuperAgers were excluded for poor image quality, the fifth SuperAger's pair was excluded and there were no other Normal Agers that met matching criteria for this SuperAger). Our final sample included 20 SuperAgers (15 female, mean age 72.1) and 20 Normal Agers (15 female, mean age 72.1). Demographic information and cognitive test data are shown in Table 1. The mean age of our SuperAgers sample was similar to Zhang and colleagues (2020) who report a mean age of 67.8 ± 6.0 years.

Image Acquisition

Whole brain T1-weighted magnetization-prepared rapid gradient echo (MPRAGE) anatomical scans were acquired sagittally (echo time (TE) = min full echo; repetition time (TR) = 2300 ms; inversion time (TI) = 900 ms; FOV = 208 x 240 x 256 mm; slice thickness

Table 2
MNI Coordinates for DMN and SN Seeds and Targets Identified Using the Harvard-Oxford Atlases.

Region	MNI coordinates		
	x	y	z
Default Mode Network			
PCC seed	1	−35	33
L AG	−47	−55	49
L SFG	−21	27	53
L dmPFC	−7	43	45
L rmPFC	−11	67	7
R AG	55	−51	39
R aMTG	57	−1	−29
R vlPFC	49	41	5
R dmPFC	7	45	45
R pgACC	3	35	15
R sgACC	3	35	−3
R rmPFC	9	67	5
R HF	29	−17	−17
Salience Network			
dAI seed	35	17	1
Bil MCC	0	3	37
R SMG	59	−31	37

Note. Montreal Neurological Institute (MNI) coordinates for the default mode network (DMN) and salience network (SN) seeds and targets created by selecting voxels for Zhang et al.'s [61] regions of interest (ROIs) within the corresponding areas defined in the Harvard-Oxford Atlases [14]. DMN and SN regions are as follows: DMN: posterior cingulate cortex (seed) (PCC), left and right angular gyrus (AG), dorsomedial prefrontal cortex (dmPFC), and rostromedial prefrontal cortex (rmPFC), left superior frontal gyrus (SFG), and right anterior middle temporal gyrus (aMTG), ventrolateral prefrontal cortex (vlPFC), pregenual and subgenual anterior cingulate cortex (pgACC/sgACC), and hippocampal formation (HF); SN: dorsal anterior insula (seed) (dAI) bilateral midcingulate cortex (MCC) and right supramarginal gyrus (SMG).

1.0 for Philips and Siemens scanners and 1.2 for GE scanners). Rs-fMRI scans were completed using an echo-planar imaging (EPI) sequence (eyes open, TR = 3000 ms, TE = 30 ms, flip angle 90°; FOV = 220 x 220 x 163 mm; slice thickness = 3.4 for Philips and GE scanners and 3.3 for Siemens scanners; 140 volumes; number of axial slices = 48; matrix = 64 x 64). For more information on ADNI's acquisition protocol, see the *ADNI3 MRI Analysis User Document* [4].

Image Preprocessing

Participant scans were downloaded from the ADNI database in DICOM format and converted to NIFTI for analysis [30]). Preprocessing and analysis were performed using FMRIB Software Library (FSL) [29]. Non-brain tissue was removed from each participant's anatomical image using the Brain Extraction Tool (BET) [49], with parameters selected for each individual based on a visual inspection of the results. Whereas most functional images had 197 volumes, those with 200 volumes were clipped to 197 volumes using the command fslroi. One image had 140 total volumes, so its pair was clipped to 140 volumes to match. Given the low sample size, we decided to include the rsfMRI with 140 volumes and compensated for the lower SNR by clipping its matched pair from the other group to 140 volumes as well. In FEAT [60], the first four volumes were removed, high pass filter was turned off, a slice timing correction was applied, spatial smoothing was performed using a 6 mm FWHM kernel, and motion correction was performed with MCFLIRT [28]. Nuisance regression included three regressors of no interest: the average global signal, the cerebrospinal fluid (CSF) signal in the lateral ventricles, and the white matter signal [61]. There have been valid criticisms of the use of the global signal as a nuisance regressor (e.g., [31]; however, it was included in this analysis in the interest of closely replicating Zhang et al. [61]. Functional images were linearly registered to standard space with FLIRT using the Montreal Neurological Institute (MNI) 152 2-mm brain standard image [29], as per Zhang and colleagues. However, in addition to linear registration, non-linear registration was performed using FNIRT [5]. We report FC results for both linearly and non-linearly registered images.

Voxelwise Functional Connectivity Analysis

Voxelwise analyses were conducted on both the linear and non-linear registered images in FEAT. Using FEAT was a different approach than Zhang and colleagues (2020), in which Pearson's correlations were calculated between the seed timecourse and each voxel's timecourse. By performing the analysis within FEAT, we were able to take advantage of its functionality (e.g., implementation of best practice for fMRI multiple comparison correction). We wanted to avoid replicating aspects of previous work that are not consistent with current best practice; however, we recognize that these deviations may make replication more difficult. *A priori* DMN and SN seed ROIs were created using coordinates identified by Zhang and colleagues (2020) (henceforth referred to as Zhang's ROIs). Spherical ROIs (4-mm radius) were created using fslmaths. These seeds were centered on the left PCC (DMN seed; MNI coordinates 1 mm, −55 mm, 17 mm) and right dAI (SN seed; MNI coordinates 36 mm, 21 mm, 1 mm). White matter and lateral ventricles were identified using the Harvard-Oxford Subcortical Atlas [14] and thresholded to 75 % probability. Global signal masks were created with BET in FEAT. The seed ROIs and the ROIs used to generate regressors of no interest were binarized using fslmaths and registered to each participant's anatomical image using applywarp. Timecourses were extracted using fslmeants. FEAT was used to generate a *z*-map displaying the voxels where FC strength was significantly different between groups (cluster-based thresholding; $z > 3.1$, $p < 0.05$).

Seed-Target ROI Functional Connectivity Analysis

Zhang and colleagues (2020) used the gray matter clusters in the masked contrast maps to identify DMN and SN targets for a seed-target ROI analysis. However, the voxelwise analysis in the current study revealed only one cluster that showed a significant difference in SuperAger-Normal Ager FC strength (Normal Agers showed greater FC strength in the white matter of precentral gyrus (PrG) in the SN analysis). Therefore, we continued with Zhang's methods by creating a 4-mm spherical ROI around the cluster identified in the voxelwise analysis (PrG *z*-peak region, MNI coordinates −41, 1, 23 mm) for a seed-target ROI analysis. For each participant, fslstats was used to extract the average parameter estimate within the PrG ROI for the SN analysis. Statistical analyses were conducted following Zhang's methods using the software jamovi [55]. An independent samples *t*-test ($p < 0.05$, 2-tailed) was performed to compare group connectivity strength between the dAI and PrG ROI, and Pearson's r ($p < 0.05$, 1-tailed) was calculated to evaluate the correlation between dAI-PrG FC strength and memory performance (positive correlations for immediate score and negative correlations for the forgetting score on the RAVLT). As per Zhang et al. [61], a false discovery rate (FDR) q of 0.05 was used to correct for multiple comparisons [7].

Since the voxelwise analysis in the current study revealed only one region with significant group differences in FC strength, we decided to conduct a second seed-target ROI analysis using the DMN and SN target ROI coordinates from Zhang et al.'s [61] ROI analysis to see if the more sensitive ROI analysis would yield significant differences in group FC strength. Spherical ROIs (4-mm radius) were created around 12 DMN targets and three SN targets (see [61]. For each participant, average parameter estimates were extracted for each target ROI. Independent samples *t*-tests were conducted to compare FC strength between groups and Pearson's r was calculated to compare correlations between FC strength and memory performance ($p < 0.05$).

While performing the seed-target ROI analysis using the target coordinates from Zhang and colleagues (2020), we noted that, when viewed on the MNI 152 template in FSL, two of the ROIs used in this analysis (left angular gyrus and right anterior middle temporal gyrus) appeared partially outside of the brain and/or outside of the regions for which they were named according to the Harvard-Oxford Cortical Atlas (see Supplementary Fig. 1). This may relate to small differences between the FSL template and the SPM2 MNI 152 template used by Zhang and colleagues (2020). Therefore, a third set of analyses were performed. The DMN and SN seed ROIs were

recreated by selecting a centrally-located voxel within the PCC and dAI areas defined in the Harvard-Oxford Cortical Atlas [14] and building 4-mm spherical ROIs around those voxels which were then binarized and registered to each participant. A new voxelwise analysis was performed using these PCC and dAI ROIs. However, no significant group differences in within network FC were identified (cluster-based thresholding; $z > 3.1$, $p < 0.05$). We continued the analysis using the same method to create new target ROIs for a third seed-target ROI analysis (selecting centrally-located voxels for Zhang's DMN and SN targets located within the corresponding regions from the Harvard-Oxford Atlases [14], Table 2). Once again, independent samples *t*-tests were performed to compare FC strength between groups, and Pearson's *r* was calculated to compare correlations between FC strength and memory performance ($p < 0.05$, corrected for multiple comparisons) were performed.

We also completed a voxelwise analysis at a less stringent threshold ($z > 2.3$, $p < 0.05$) which was more comparable to the statistical approach in Zhang and colleagues (2020). Because the goal of this analysis was to better match with Zhang and colleagues' (2020) analysis, we considered the less stringent threshold only for the linearly-registered data and Zhang and colleagues' (2020) ROI coordinates.

Results

SuperAgers and Normal Agers Demonstrate Similar DMN and SN FC Strength

We ran voxelwise analyses using both linear and non-linear registration to standard space. For both these registrations, we used both Zhang and colleagues (2020) seed regions and seed regions derived from the Harvard-Oxford Atlas, for a total of eight voxelwise analyses. The group average FC maps were similar across all eight analyses. Supplementary Fig. 2 depicts the DMN for both groups and Supplementary Fig. 3 depicts the SN for both groups, for the analysis using linear registration and Zhang and colleagues' (2020) seed region. Contrary to the findings of Zhang and colleagues (2020), of the eight voxelwise analyses we ran, only one analysis showed significantly different connectivity strength between groups, and the difference was restricted to one region (Fig. 1). A region overlapping the white matter of the left precentral gyrus (Fig. 1) showed stronger Normal Ager FC with the SN seed ($p < 0.05$). This finding was restricted to the linear registered images; no between-group FC differences were observed for the non-linear registered images. A seed-target analysis of dAI-PrG connectivity revealed a significant group difference in connectivity strength ($t(36.3) = 3.23$, $p = 0.003$).

The results of the analysis using a less stringent statistical threshold can be found in Supplementary Fig. 4.

The results of the second and third seed-target ROI analyses are shown in Figs. 2 and 3. Zhang's ROIs (Table 1) resulted in only one significant group difference where Normal Agers showed stronger connectivity between the SN seed and the right midcingulate cortex (MCC) ($t(33.42) = 2.11$, $p = 0.042$); however, this difference did not survive multiple comparisons (FDR, $q = 0.05$ [7]). The new ROIs defined based on the Harvard-Oxford Atlas (Table 2) resulted in two significant group differences in DMN connectivity strength where Normal Agers showed stronger connectivity between the PCC and the left rostromedial prefrontal cortex (rmPFC) ($t(34.7) = 2.72$, $p = 0.010$) and right rmPFC ($t(28.0) = 2.68$, $p = 0.012$; again however, these differences did not survive multiple comparisons ($q > 0.05$).

Correlations between within network connectivity strength and memory performance

Table 3 shows the correlations between DMN and SN FC strength and memory performance on the RAVLT. In two of Zhang's DMN regions and one SN region, there were significant correlations between FC strength and the RAVLT immediate score (uncorrected *p*-value significance); however, these correlations did not survive multiple comparisons (FDR, $q = 0.05$ [7]). FC strength in all remaining regions did not significantly correlate with either RAVLT memory score. The three regions from Zhang's ROIs that correlated with

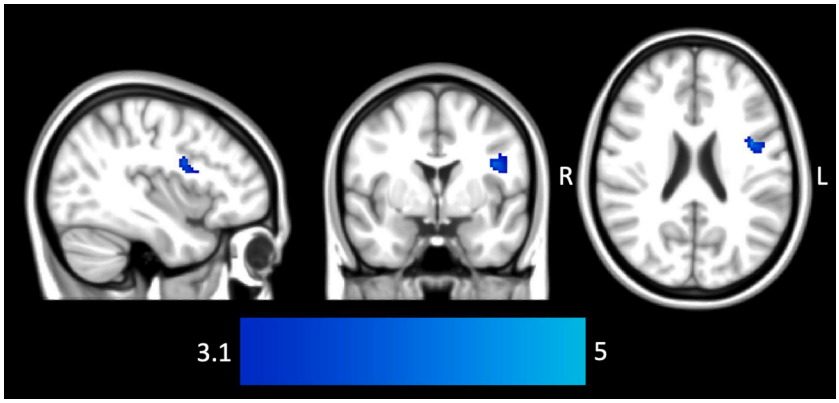

Fig. 1. Voxels Showing Stronger Connectivity Strength with Salience Network Seed in Normal Agers. *Note*. Voxels in which Normal Agers showed significantly stronger functional connectivity with the dorsal anterior insula (dAI) (salience network seed) ($3.1 < z < 5$, $p < 0.05$). This region, revealed in the voxelwise analysis of participants' linear registered images, was localized to the white matter of the precentral gyrus (PrG) (left).

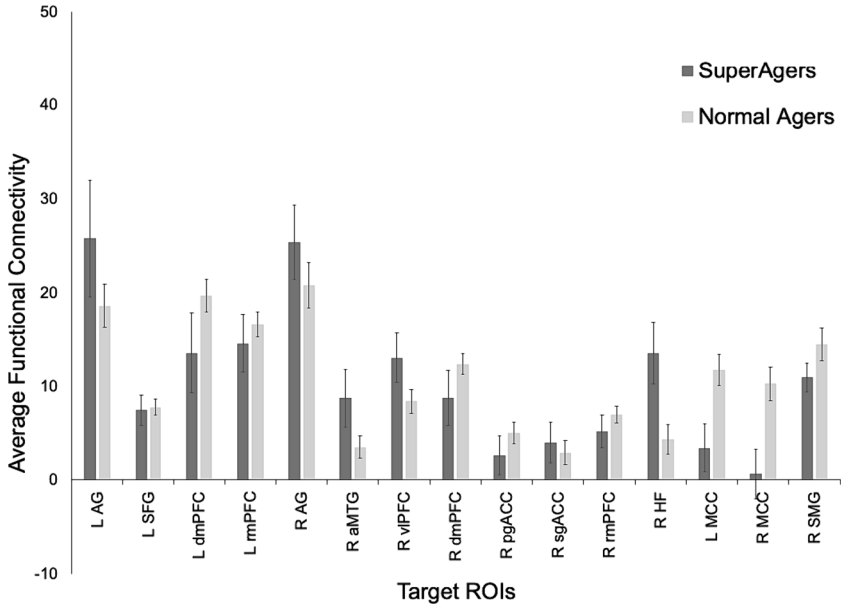

Fig. 2. Intrinsic Functional Connectivity Strength in Default Mode and Salience Networks for Regions of Interest created Using Coordinates Reported by Zhang et al. (2020). *Note*. Bars demonstrate the differences in average SuperAger and Normal Ager intrinsic functional connectivity strength within the default mode (DMN) and salience (SN) networks. Error bars represent the standard error of the mean. Regions of interest were created using coordinates given by Zhang et al. (2020). Regions are as follows: DMN: angular gyrus (AG), superior frontal gyrus (SFG), dorsomedial prefrontal cortex (dmPFC), rostromedial prefrontal cortex (rmPFC), anterior middle temporal gyrus (aMTG), ventrolateral prefrontal cortex (vlPFC), pregenual and subgenual anterior cingulate cortex (pgACC/sgACC), and hippocampal formation (HF); SN: midcingulate cortex (MCC) and supramarginal gyrus (SMG).

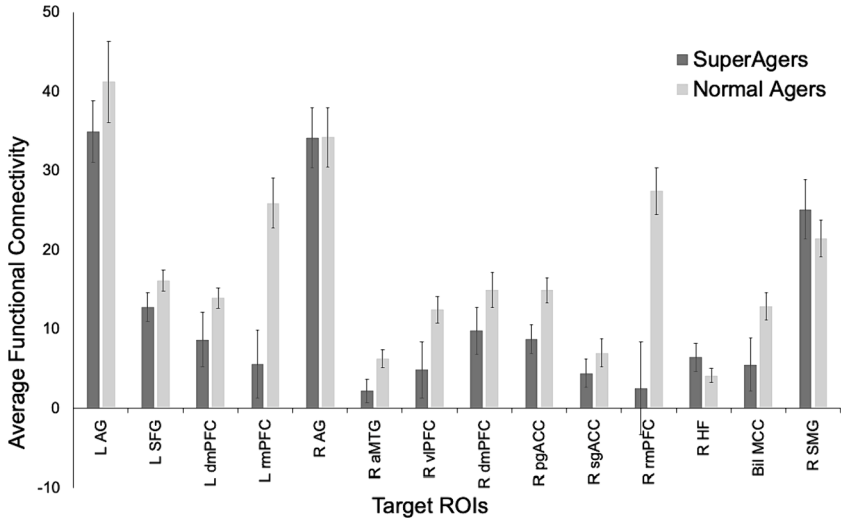

Fig. 3. Intrinsic Functional Connectivity Strength in Default Mode and Salience Networks for Regions of Interest Created Using the Harvard-Oxford Atlases. *Note*. Bars demonstrate the differences in average SuperAger and Normal Ager intrinsic functional connectivity strength within the default mode (DMN) and salience (SN) networks. Error bars represent the standard error of the mean. Regions of interest were created using network regions defined by the Harvard Oxford Atlases. Regions are as follows: DMN: angular gyrus (AG), superior frontal gyrus (SFG), dorsomedial prefrontal cortex (dmPFC), rostromedial prefrontal cortex (rmPFC), anterior middle temporal gyrus (aMTG), ventrolateral prefrontal cortex (vlPFC), pregenual and subgenual anterior cingulate cortex (pgACC/sgACC), and hippocampal formation (HF); SN: midcingulate cortex (MCC) and supramarginal gyrus (SMG).

Table 3
Associations Between Functional Connectivity Strength and Memory Performance.

Target Region	RAVLT Immediate Score			RAVLT Forgetting Score	
	r	*p*		*r*	*p*
SN - cluster identified in voxelwise analysis					
PrG	-0.43	0.005	*	0.12	0.451
DMN - Zhang ROIs					
L AG	0.26	0.099		-0.16	0.337
L SFG	0.04	0.823		0.03	0.841
L dmPFC	-0.01	0.952		0.08	0.613
L rmPFC	-0.06	0.734		0.12	0.461
R AG	0.24	0.130		-0.09	0.575
R aMTG	0.35	0.028	*	-0.15	0.359
R vlPFC	0.22	0.168		-0.02	0.905
R dmPFC	0.03	0.867		0.05	0.737
R pgACC	0.08	0.630		-0.06	0.713
R sgACC	0.25	0.122		-0.22	0.165
R rmPFC	0.01	0.961		-0.06	0.693
R HF	0.42	0.007	*	-0.10	0.555
SN - Zhang ROIs					
L MCC	-0.30	0.058		0.24	0.134
R MCC	-0.34	0.031	*	0.24	0.139
R SMG	-0.07	0.676		-0.06	0.721
DMN - Harvard-Oxford ROIs					
L AG	-0.11	0.752		0.10	0.728
L SFG	-0.06	0.634		0.20	0.893
L dmPFC	-0.09	0.711		0.21	0.902
L rmPFC	-0.27	0.952		0.30	0.969
R AG	0.04	0.404		0.00	0.503
R aMTG	-0.14	0.804		0.21	0.900
R vlPFC	-0.10	0.739		0.09	0.714
R dmPFC	-0.11	0.755		0.21	0.909
R pgACC	-0.31	0.976		0.27	0.955
R sgACC	-0.02	0.539		-0.13	0.218
R rmPFC	-0.28	0.962		0.26	0.947
R HF	0.25	0.062		-0.01	0.477
SN - Harvard-Oxford ROIs					
Bil MCC	-0.18	0.870		0.15	0.821
R SMG	0.25	0.057		-0.17	0.152

Note. Associations between within network functional connectivity strength in the default mode network (DMN) and salience network (SN) and memory performance on the Rey Auditory Verbal Learning Test (RAVLT). r = Pearson's correlation coefficient. p = 1-tailed significance (positive correlations) for RAVLT immediate (sum of words recalled after five learning trials; p = 1-tailed significance (negative correlations) for RAVLT forgetting (words recalled on trial five minus words recalled after a delay). Regions of interest (ROIs) are as follows: precentral gyrus (PrG), angular gyrus (AG), superior frontal gyrus (SFG), dorsomedial prefrontal cortex (dmPFC), rostromedial prefrontal cortex (rmPFC), anterior middle temporal gyrus (aMTG), ventrolateral prefrontal cortex (vlPFC), pregenual and subgenual anterior cingulate cortex (pgACC/sgACC), and hippocampal formation (HF); SN: midcingulate cortex (MCC) and supramarginal gyrus (SMG). ROIs created using coordinates from Zhang et al. [61] and the Harvard-Oxford Atlases [14].
* $p < 0.05$.

memory performance were R aMTG: $r = 0.35$, $p = 0.028$; R HF: $r = 0.42$, $p = 0.007$; R MCC: $r = 0.34$, $p = 0.031$; all uncorrected p-values.

Discussion

We were unable to replicate the findings of Zhang et al. [61], that SuperAgers show stronger functional connectivity within default mode and salience networks, and that functional connectivity strength in these networks positively correlates with memory performance, from a sample of SuperAgers and Normal Agers identified within the ADNI database. Our results indicated that SuperAgers generally do not demonstrate significantly stronger FC within the DMN or SN, and that FC strength within these networks does not correlate with memory performance. The only significant difference in group FC strength identified in the current study showed that Normal Agers had stronger FC between the SN seed region and a region localized in the white matter of the PrG, and SN FC strength in this region was negatively correlated with memory performance. It is possible that this white matter region is involved in connections to brain regions more commonly associated with memory. However, we note that the higher SN FC connectivity in the white matter of the PrG was only observed when linear image registration was used, and that no FC differences were observed between groups when non-linear registration was used. It is thus possible that the finding in the white matter of the PrG was related to registration errors.

The replication crisis in psychology has been a major topic of discussion over the last decade. Large numbers of psychological studies have failed to replicate. Maxwell et al. [34] suggest that many unsuccessful replications can be credited to low statistical power and small sample sizes. As the current study included a sample size of 40 participants and the original study by Zhang et al. [61] also

included 40 older adults, it is possible that our failure to replicate could be attributed to low statistical power and small sample size in both our study and the original study. See Maxwell et al. [34] and Nosek et al. [37] for further reading on the challenges of replication.

Methodological differences between the current study and Zhang and colleagues

Group definitions. Zhang et al. [61] used the CVLT to measure episodic memory performance, the current study was restricted to using the RAVLT as this measure is available in the ADNI database. Furthermore, where Zhang and colleagues (2020) used the delayed recall score in their definition of SuperAging, ADNI does not provide an RAVLT delayed recall score. Thus, the current study used a forgetting score which is the number of words recalled on the last learning trial minus the words recalled after the delay. Given that many studies of SuperAgers use RAVLT scores or composite scores including RAVLT and report significant differences [12], we do not think use of the RAVLT limited our ability to detect differences. We note that our groups differed significantly in their RAVLT performance.

MRI data and analysis. Zhang's study included a sample of younger individuals to directly compare older individuals' cognitive performance and FC strength. The ADNI database only includes individuals aged 55+, thus we did not have MRI data from a young adult group. Data analysis differences included using FEAT instead of Pearson's correlation and correcting for multiple comparisons. We opted to make changes in the data analysis pipeline in order to conform with current best practices, but we recognize that these decisions likely contributed to the discrepancies we observed between our results and Zhang and colleagues (2020) results.

An additional limitation relates to potential heterogeneity associated with scanner manufacturer and site. The case matching we performed ensured that SuperAgers were matched with a Normal Ager whose data was collected using a scanner from the same manufacturer. However, due to the large number of sites included (23), which was required to ensure an adequate sample size of SuperAgers, it was not practical to account for scanner site in the analysis. This is an expected limitation of using large, freely available databases. Future work using larger sample sizes and/or data collected for the purpose of studying SuperAgers will help mitigate heterogeneity associated with scanner manufacturer and site.

Similarities to Previous Results

Overall, we clearly did not replicate the results of Zhang et al. [61] in that we did not find widespread regions of increased functional connectivity in SuperAgers relative to Normal Agers, nor did we find numerous regions with FC that were correlated with memory test performance. However, we did observe some similarities between our results and the previous study. Specifically, we observed several marginal effects that resembled Zhang and colleagues (2020) results. For example, the correlation between the right HF FC within the DMN and the RAVLT immediate score approached significance in our study; Zhang and colleagues (2020) reported a similar correlation (bivariate Pearson Correlation, 1-tailed, FDR-corrected, $q < 0.05$) between the right HF FC and CVLT verbal recall $r = 0.34$, $p = 0.02$) as significant. We posit that our study provides some indication that some of Zhang and colleagues (2020) findings might be observed in future studies, perhaps with a larger sample (see below for more discussion on sample size). Beyond evaluating our results relative to Zhang and colleagues (2020), our findings were unusual in that most fMRI studies comparing SuperAgers with Normal Agers report activation or FC differences [12] or are able to distinguish between SuperAgers and Normal Agers on the basis of FC using machine learning [40].

Limitations and future directions

Variability in SuperAger Definitions and Terminology

A lack of consensus on SuperAger definition currently limits the field's ability to integrate results across studies. There is considerable variation in the age range used to define SuperAgers (ranging from ages 80+ [9,20,19,18,17,25,42], 70+ [24], 60+ [11], and between the ages of 68–74 [32] and 60–80 [53,61]. The current study used an age range of 60+, whereas Zhang and colleagues used an age range of 60–80. We had only three participants in each group over age 80, and no participant over age 87. Further, the mean age of our SuperAger sample (72.1 ± 6.8 years) was similar to that of Zhang and colleagues' (2020) of 67.8 ± 6.0 years, so we do not expect the differences in age to impact the replication substantially. In general, age-related changes in functional connectivity will be impacted by choice of SuperAger age criteria. For example, Staffaroni and colleagues (2018) found a trend toward increased within-network DMN FC between the ages of 50–66 followed by a significantly accelerating decline after the age of 74. Therefore, differences in FC between SuperAgers and Normal Agers may be greater after the age of 74. Furthermore, the ages of the younger comparison groups and/or normative in SuperAging studies vary drastically (from ages 18–32, to ages 30–44, as far as individuals in their 50s to 60s). Thus, "SuperAgers" in one study may not qualify for SuperAging in another study due to their age and/or memory performance, yet they use the same term.

Small Sample Sizes and Volunteer Bias in SuperAging Research

Small sample sizes are a limitation in SuperAging studies. Most SuperAging studies include a sample of older individuals (combined SuperAgers and Normal Agers) of < 100. Larger sample sizes are likely needed to adequately power studies. However, it may be difficult to study large samples of SuperAgers due to low prevalence rates. Although many SuperAging studies have apparently high prevalence rates (e.g., 30.9 % in Dang et al. [11], 38.6 % in Zhang et al. [61], these studies are not designed specifically to estimate

prevalence. In contrast, a study which did report SuperAging prevalence estimated 6.9 % of Australian older adults are SuperAgers [32]. We estimate that 9.0 % of the cognitively healthy controls in the ADNI database are SuperAgers (35 SuperAgers out of 391 ADNI participants with fMRI, RAVLT, and TMT-B data available). Furthermore, some SuperAging studies, including Zhang et al. [61], do not adequately describe their recruitment methods and have a high risk of bias in patient selection according to the Quality Assessment of Diagnostic Accuracy Studies-2 (QUADAS-2) [12]. Research into aging is complicated with volunteer bias as studies have difficulty recruiting and retaining older individuals due to factors such as transportation problems, disability/impaired mobility, illness, and death [16]. Thus, healthier and more physically able participants are more likely to volunteer for and complete studies. The title of the study and/or research topic might also attract different types of participants (e.g., individuals with a family history of AD may be more interested in volunteering for ADNI, whereas individuals with a family history of longevity may be more interested in volunteering for a study explicitly on SuperAgers). It is likely that considerable sampling and/or volunteer bias is contributing to the high SuperAging prevalence rates that are reported in some studies. More work needs to be done to estimate prevalence accurately. Furthermore, the SuperAging definition used can affect the number of SuperAgers identified.

Conclusions

The degree to which FC of the DMN and SN differ between SuperAgers and Normal Agers remains an open question. Larger studies are needed to understand the demographics and backgrounds of SuperAgers, as well as to increase statistical power for biomarker investigations. In addition, longitudinal studies will be key to understanding the mechanisms of SuperAging. Longitudinal data will allow us to evaluate whether SuperAgers have unusually good episodic memory and functional connectivity throughout life, versus preserving normal midlife levels of episodic memory and functional connectivity. Consensus on SuperAger definition among research groups is critical for meaningful comparisons of future studies. Ultimately, research into the mechanisms of SuperAging has significant potential for identifying interventions that may improve quality of life throughout aging.

CRediT authorship contribution statement

Haley E. Keenan: Conceptualization, Data curation, Formal analysis, Methodology, Visualization, Writing – original draft, Writing – review & editing. **Alexis Czippel:** Conceptualization, Data curation, Writing – review & editing. **Sepideh Heydari:** Conceptualization, Writing – review & editing. **Jodie R. Gawryluk:** Conceptualization, Data curation, Formal analysis, Methodology, Resources, Supervision, Writing – review & editing. **Erin L. Mazerolle:** Conceptualization, Data curation, Formal analysis, Funding acquisition, Methodology, Project administration, Resources, Supervision, Visualization, Writing – original draft, Writing – review & editing.

Declaration of competing interest

The authors declare that they have no known competing financial interests or personal relationships that could have appeared to influence the work reported in this paper.

Acknowledgements

This work was supported by Research Nova Scotia [no grant number]; and the Natural Sciences and Engineering Research Council of Canada (NSERC) [grant number RGPIN/21-02393]. Data collection and sharing for this project was funded by the Alzheimer's Disease Neuroimaging Initiative (ADNI) (National Institutes of Health Grant U01 AG024904) and DOD ADNI (Department of Defense award number W81XWH-12-2-0012). ADNI is funded by the National Institute on Aging, the National Institute of Biomedical Imaging and Bioengineering, and through generous contributions from the following: AbbVie, Alzheimer's Association; Alzheimer's Drug Discovery Foundation; Araclon Biotech; BioClinica, Inc.; Biogen; Bristol-Myers Squibb Company; CereSpir, Inc.; Cogstate; Eisai Inc.; Elan Pharmaceuticals, Inc.; Eli Lilly and Company; EuroImmun; F. Hoffmann-La Roche Ltd and its affiliated company Genentech, Inc.; Fujirebio; GE Healthcare; IXICO Ltd.;Janssen Alzheimer Immunotherapy Research & Development, LLC.; Johnson & Johnson Pharmaceutical Research & Development LLC.; Lumosity; Lundbeck; Merck & Co., Inc.; Meso Scale Diagnostics, LLC.; NeuroRx Research; Neurotrack Technologies; Novartis Pharmaceuticals Corporation; Pfizer Inc.; Piramal Imaging; Servier; Takeda Pharmaceutical Company; and Transition Therapeutics. The Canadian Institutes of Health Research is providing funds to support ADNI clinical sites in Canada. Private sector contributions are facilitated by the Foundation for the National Institutes of Health (www.fnih.org). The grantee organization is the Northern California Institute for Research and Education, and the study is coordinated by the Alzheimer's Therapeutic Research Institute at the University of Southern California. ADNI data are disseminated by the Laboratory for Neuro Imaging at the University of Southern California.

Appendix A. Supplementary data

Supplementary data to this article can be found online at https://doi.org/10.1016/j.nbas.2024.100114.

References

[1] Allen E, Erhardt E, Damaraju E, Gruner W, Segall J, Silva R, et al. A baseline for the multivariate comparison of resting-state networks. Front Syst Neurosci 2011; 5. https://www.frontiersin.org/articles/10.3389/fnsys.2011.00002.

[2] Alzheimer's Disease Neuroimaging Initiative. (n.d.). ADNI2 procedures manual. https://adni.loni.usc.edu/wp-content/uploads/2008/07/adni2-procedures-manual.pdf.

[3] Alzheimer's Disease Neuroimaging Initiative. (2017). ADNI3 Procedures Manual Version 3.0. https://adni.loni.usc.edu/wp-content/uploads/2012/10/ADNI3-Procedures-Manual_v3.0_20170627.pdf.

[4] Alzheimer's Disease Neuroimaging Initiative. (2018). Alzheimer's Disease Neuro Imaging III (ADNI3) MRI Analysis User Document. https://adni.loni.usc.edu/wp-content/themes/freshnews-dev-v2/documents/mri/ADNI3_MRI_Analysis_Manual_20180202.pdf.

[5] Andersson, J. L. R., Jenkinson, M., & Smith, S. (2010). Non-linear registration aka spatial normalisation FMRIB technical report TR07JA2.

[6] Andrews-Hanna JR, Snyder AZ, Vincent JL, Lustig C, Head D, Raichle ME, et al. Disruption of large-scale brain systems in advanced aging. Neuron 2007;56(5): 924–35. https://doi.org/10.1016/j.neuron.2007.10.038.

[7] Benjamini Y, Hochberg Y. Controlling the false discovery rate: a practical and powerful approach to multiple testing. J R Stat Soc 1995;57:289–300. https://doi.org/10.1111/j.2517-6161.1995.tb02031.x.

[8] Buckner RL, Andrews-Hanna JR, Schacter DL. The brain's default network: anatomy, function, and relevance to disease. Ann N Y Acad Sci 2008;1124(1):1–38. https://doi.org/10.1196/annals.1440.011.

[9] Cook AH, Sridhar J, Ohm D, Rademaker A, Mesulam M-M, Weintraub S, et al. Rates of cortical atrophy in adults 80 years and older with superior vs average episodic memory. JAMA 2017;317(13):1373–5. https://doi.org/10.1001/jama.2017.0627.

[10] Damoiseaux JS, Beckmann CF, Arigita EJS, Barkhof F, Scheltens Ph, Stam CJ, et al. Reduced resting-state brain activity in the "default network" in normal aging. Cereb Cortex 2008;18(8):1856–64. https://doi.org/10.1093/cercor/bhm207.

[11] Dang, C., Yassi, N., Harrington, K. D., Xia, Y., Lim, Y. Y., Ames, D., Laws, S. M., Hickey, M., Rainey-Smith, S., Sohrabi, H. R., Doecke, J. D., Fripp, J., Salvado, O., Snyder, P. J., Weinborn, M., Villemagne, V. L., Rowe, C. C., Masters, C. L., Maruff, P., & AIBL Research Group. (2019). Rates of age- and amyloid β-associated cortical atrophy in older adults with superior memory performance. Alzheimer's & Dementia, 11, 566–575. doi: 10.1016/j.dadm.2019.05.005.

[12] de Godoy LL, Alves CAPF, Saavedra JSM, Studart-Neto A, Nitrini R, da Costa Leite C, et al. Understanding brain resilience in superagers: a systematic review. Neuroradiology 2021;63(5):663–83. https://doi.org/10.1007/s00234-020-02562-1.

[13] Delis, D. C., Kramer, J. H., Kaplan, E., & Thompkins, B. A. O. (1987). *CVLT: California Verbal Learning Test-adult version: Manual*. Psychological Corporation.

[14] Desikan RS, Ségonne F, Fischl B, Quinn BT, Dickerson BC, Blacker D, et al. An automated labeling system for subdividing the human cerebral cortex on MRI scans into gyral based regions of interest. Neuroimage 2006;31(3):968–80. https://doi.org/10.1016/j.neuroimage.2006.01.021.

[15] Esposito F, Aragri A, Pesaresi I, Cirillo S, Tedeschi G, Marciano E, et al. Independent component model of the default-mode brain function: combining individual-level and population-level analyses in resting-state fMRI. Magn Reson Imaging 2008;26(7):905–13. https://doi.org/10.1016/j.mri.2008.01.045.

[16] Forsat ND, Palmowski A, Palmowski Y, Boers M, Buttgereit F. Recruitment and retention of older people in clinical research: a systematic literature review. J Am Geriatr Soc 2020;68(12):2955–63. https://doi.org/10.1111/jgs.16875.

[17] Gefen T, Kawles A, Makowski-Woidan B, Engelmeyer J, Ayala I, Abbassian P, et al. Paucity of entorhinal cortex pathology of the Alzheimer's type in SuperAgers with superior memory performance. Cereb Cortex 2021;31(7):3177–83. https://doi.org/10.1093/cercor/bhaa409.

[18] Gefen T, Papastefan ST, Rezvanian A, Bigio EH, Weintraub S, Rogalski E, et al. Von economo neurons of the anterior cingulate across the lifespan and in Alzheimer's disease. Cortex 2018;99:69–77. https://doi.org/10.1016/j.cortex.2017.10.015.

[19] Gefen T, Peterson M, Papastefan ST, Martersteck A, Whitney K, Rademaker A, et al. Morphometric and histologic substrates of cingulate integrity in elders with exceptional memory capacity. J Neurosci 2015;35(4):1781–91. https://doi.org/10.1523/JNEUROSCI.2998-14.2015.

[20] Gefen T, Shaw E, Whitney K, Martersteck A, Stratton J, Rademaker A, et al. Longitudinal neuropsychological performance of cognitive SuperAgers. J Am Geriatr Soc 2014;62(8):1598–600. https://doi.org/10.1111/jgs.12967.

[21] Goulden N, Khusnulina A, Davis NJ, Bracewell RM, Bokde AL, McNulty JP, et al. The salience network is responsible for switching between the default mode network and the central executive network: replication from DCM. Neuroimage 2014;99:180–90. https://doi.org/10.1016/j.neuroimage.2014.05.052.

[22] Greicius MD, Krasnow B, Reiss AL, Menon V. Functional connectivity in the resting brain: a network analysis of the default mode hypothesis. Proc Natl Acad Sci 2003;100(1):253–8. https://doi.org/10.1073/pnas.0135058100.

[23] Harada CN, Natelson Love MC, Triebel K. Normal cognitive aging. Clin Geriatr Med 2013;29(4):737–52. https://doi.org/10.1016/j.cger.2013.07.002.

[24] Harrison TM, Maass A, Baker SL, Jagust WJ. Brain morphology, cognition, and β-amyloid in older adults with superior memory performance. Neurobiol Aging 2018;67:162–70. https://doi.org/10.1016/j.neurobiolaging.2018.03.024.

[25] Harrison TM, Weintraub S, Mesulam M-M, Rogalski E. Superior memory and higher cortical volumes in unusually successful cognitive aging. J Int Neuropsychol Soc 2012;18(6):1081–5. https://doi.org/10.1017/S1355617712000847.

[26] Hayes JM, Tang L, Viviano RP, van Rooden S, Ofen N, Damoiseaux JS. Subjective memory complaints are associated with brain activation supporting successful memory encoding. Neurobiol Aging 2017;60:71–80. https://doi.org/10.1016/j.neurobiolaging.2017.08.015.

[27] Herting MM, Nagel BJ. Differences in brain activity during a verbal associative memory encoding task in high- and low-fit adolescents. J Cogn Neurosci 2013;25 (4):595–612. https://doi.org/10.1162/jocn_a_00344.

[28] Jenkinson M, Bannister P, Brady M, Smith S. Improved optimization for the robust and accurate linear registration and motion correction of brain images. Neuroimage 2002;17(2):825–41. https://doi.org/10.1016/s1053-8119(02)91132-8.

[29] Jenkinson M, Beckmann CF, Behrens TEJ, Woolrich MW, Smith SM. FSL. NeuroImage 2012;62(2):782–90. https://doi.org/10.1016/j.neuroimage.2011.09.015.

[30] Li X, Morgan PS, Ashburner J, Smith J, Rorden C. The first step for neuroimaging data analysis: DICOM to NIfTI conversion. J Neurosci Methods 2016;264: 47–56. https://doi.org/10.1016/j.jneumeth.2016.03.001.

[31] Liu TT, Nalci A, Falahpour M. The global signal in fMRI: nuisance or information? Neuroimage 2017;150:213–29. https://doi.org/10.1016/j.neuroimage.2017.02.036.

[32] Maccora J, Peters R, Anstey KJ. Gender differences in superior-memory SuperAgers and associated factors in an australian cohort. J Appl Gerontol 2021;40(4): 433–42. https://doi.org/10.1177/0733464820902943.

[33] Marstaller L, Williams M, Rich A, Savage G, Burianová H. Aging and large-scale functional networks: white matter integrity, gray matter volume, and functional connectivity in the resting state. Neuroscience 2015;290:369–78. https://doi.org/10.1016/j.neuroscience.2015.01.049.

[34] Maxwell SE, Lau MY, Howard GS. Is psychology suffering from a replication crisis? what does "failure to replicate" really mean? Am Psychol 2015;70(6): 487–98. https://doi.org/10.1037/a0039400.

[35] Mazoyer B, Zago L, Mellet E, Bricogne S, Etard O, Houdé O, et al. Cortical networks for working memory and executive functions sustain the conscious resting state in man. Brain Res Bull 2001;54(3):287–98. https://doi.org/10.1016/S0361-9230(00)00437-8.

[36] Menon V, Uddin LQ. Saliency, switching, attention and control: a network model of insula function. Brain Struct Funct 2010;214(5–6):655–67. https://doi.org/10.1007/s00429-010-0262-0.

[37] Nosek BA, Hardwicke TE, Moshontz H, Allard A, Corcker KS, Dreber A, et al. Replicability, robustness, and reproducibility in psychological science. Annu Rev Psychol 2022;73:719–48. https://doi.org/10.1146/annurev-psych-020821-114157.

[38] Onoda K, Ishihara M, Yamaguchi S. Decreased functional connectivity by aging is associated with cognitive decline. J Cogn Neurosci 2012;24(11):2186–98. https://doi.org/10.1162/jocn_a_00269.

[39] Oschmann M, Gawryluk JR. A longitudinal study of changes in resting-state functional magnetic resonance imaging functional connectivity networks during healthy aging. Brain Connect 2020;10(7):377–84. https://doi.org/10.1089/brain.2019.0724.

[40] Park C, Kim BR, Park HK, Lim SM, Kim E, Jeong JH, et al. Predicting superagers by machine learning classification based on the functional brain connectome using resting-state functional magnetic resonance imaging. Cereb Cortex 2022;32(19):4183–90. https://doi.org/10.1093/cercor/bhab474.

[41] Raichle ME, MacLeod AM, Snyder AZ, Powers WJ, Gusnard DA, Shulman GL. A default mode of brain function. Proc Natl Acad Sci 2001;98(2):676–82. https://doi.org/10.1073/pnas.98.2.676.
[42] Rogalski EJ, Gefen T, Shi J, Samimi M, Bigio E, Weintraub S, et al. Youthful memory capacity in old brains: anatomic and genetic clues from the northwestern SuperAging project. J Cogn Neurosci 2013;25(1):29–36. https://doi.org/10.1162/jocn_a_00300.
[43] Schmidt M. Rey auditory verbal Learning test: RAVLT: a handbook. Western Psychological Services; 1996.
[44] Seeley WW. The salience network: a neural system for perceiving and responding to homeostatic demands. J Neurosci 2019;39(50):9878–82. https://doi.org/10.1523/JNEUROSCI.1138-17.2019.
[45] Seeley WW, Menon V, Schatzberg AF, Keller J, Glover GH, Kenna H, et al. Dissociable intrinsic connectivity networks for salience processing and executive control. J Neurosci 2007;27(9):2349–56. https://doi.org/10.1523/JNEUROSCI.5587-06.2007.
[46] Sestieri C, Corbetta M, Romani GL, Shulman GL. Episodic memory retrieval, parietal cortex, and the default mode network: functional and topographic analyses. J Neurosci 2011;31(12):4407–20. https://doi.org/10.1523/JNEUROSCI.3335-10.2011.
[47] Shapira-Lichter I, Oren N, Jacob Y, Gruberger M, Hendler T. Portraying the unique contribution of the default mode network to internally driven mnemonic processes. Proc Natl Acad Sci 2013;110(13):4950–5. https://doi.org/10.1073/pnas.1209888110.
[48] Shulman GL, Fiez JA, Corbetta M, Buckner RL, Miezin FM, Raichle ME, et al. Common blood flow changes across visual tasks: II. decreases in cerebral cortex. J Cogn Neurosci 1997;9(5):648–63. https://doi.org/10.1162/jocn.1997.9.5.648.
[49] Smith SM. Fast robust automated brain extraction. Hum Brain Mapp 2002;17(3):143–55. https://doi.org/10.1002/hbm.10062.
[50] Sridharan D, Levitin DJ, Menon V. A critical role for the right fronto-insular cortex in switching between central-executive and default-mode networks. Proc Natl Acad Sci 2008;105(34):12569–74. https://doi.org/10.1073/pnas.0800005105.
[51] Staffaroni AM, Brown JA, Casaletto KB, Elahi FM, Deng J, Neuhaus J, et al. The longitudinal trajectory of default mode network connectivity in healthy older adults varies as a function of age and is associated with changes in episodic memory and processing speed. J Neurosci 2018;38(11):2809–17. https://doi.org/10.1523/JNEUROSCI.3067-17.2018.
[52] Strauss E, Sherman EMS, Spreen O. A compendium of neuropsychological tests: administration, norms, and commentary. Oxford University Press; 2006.
[53] Sun FW, Stepanovic MR, Andreano J, Barrett LF, Touroutoglou A, Dickerson BC. Youthful brains in older adults: preserved neuroanatomy in the default mode and salience networks contributes to youthful memory in SuperAging. J Neurosci 2016;36(37):9659–68. https://doi.org/10.1523/JNEUROSCI.1492-16.2016.
[54] Taylor KS, Seminowicz DA, Davis KD. Two systems of resting state connectivity between the insula and cingulate cortex. Hum Brain Mapp 2009;30(9):2731–45. https://doi.org/10.1002/hbm.20705.
[55] The jamovi project. (2023). *Jamovi* (2.3) [Computer software]. https://www.jamovi.org.
[56] Tombaugh T. Trail making test a and B: normative data stratified by age and education. Arch Clin Neuropsychol 2004;19(2):203–14. https://doi.org/10.1016/S0887-6177(03)00039-8.
[57] Varangis, E., Habeck, C. G., Razlighi, Q. R., & Stern, Y. (2019). The effect of aging on resting state connectivity of predefined networks in the brain. Frontiers in Aging Neuroscience, 11. https://www.frontiersin.org/articles/10.3389/fnagi.2019.00234.
[58] Wang L, LaViolette P, O'Keefe K, Putcha D, Bakkour A, Van Dijk KRA, et al. Intrinsic connectivity between the hippocampus and posteromedial cortex predicts memory performance in cognitively intact older individuals. Neuroimage 2010;51(2):910–7. https://doi.org/10.1016/j.neuroimage.2010.02.046.
[59] Ward AM, Mormino EC, Huijbers W, Schultz AP, Hedden T, Sperling RA. Relationships between default-mode network connectivity, medial temporal lobe structure, and age-related memory deficits. Neurobiol Aging 2015;36(1):265–72. https://doi.org/10.1016/j.neurobiolaging.2014.06.028.
[60] Woolrich MW, Ripley BD, Brady M, Smith SM. Temporal autocorrelation in univariate linear modeling of FMRI data. Neuroimage 2001;14(6):1370–86. https://doi.org/10.1006/nimg.2001.0931.
[61] Zhang J, Andreano JM, Dickerson BC, Touroutoglou A, Barrett LF. Stronger functional connectivity in the default mode and salience networks is associated with youthful memory in SuperAging. Cereb Cortex 2020;30(1):72–84. https://doi.org/10.1093/cercor/bhz071.
[62] Zonneveld HI, Pruim RHR, Bos D, Vrooman HA, Muetzel RL, Hofman A, et al. Patterns of functional connectivity in an aging population: the Rotterdam study. Neuroimage 2019;189:432–44. https://doi.org/10.1016/j.neuroimage.2019.01.041.